Chapter 4

Polyethylene/polypropylene/alkali treated-hemp fiber based packaging film

This chapter deals with optimization of alkali-treated hemp fiber incorporated polyethylene/polypropylene film using response surface methodology for green packaging applications that was characterized by FTIR analysis, SEM analysis, XRD analysis, WVTR, WVP, contact angle, tensile test, elongation test, impact test, and optical characteristic test.

4.1 Introduction

Extensive use of non-biodegradable materials such as polystyrene, polyvinyl alcohol, polypropylene, polyamide, polyethylene, polyvinyl chloride, and polyethylene terephthalate for numerous applications such as packaging, furniture, and automotive parts are a daily need of human beings. In present context, the global fabrication of polymers is reported to be about 322 million tons (2015) (Dixit and Yadav, 2019a). However, upswing needs also result in the non-biodegradable disposal crisis. So many researchers all over the world are trying to develop an inexpensive, efficient and environment-friendly way to resolve the non-biodegradable disposal crisis. On the other side, natural fibers with cellulosic strong fiber property are abundantly available that are biodegradable too (Bourmaud and Baley, 2007; Bourmaud and Baley, 2009). Hence utilization of natural fibers in composite preparation is a promising technique of the modern world.

Environmental aspects and economic benefits encourage various researchers to synthesize a polymer composites blended with natural fiber composites for several

green applications (Singh et al., 2017; Youssef et al., 2015). Many authors have developed robust composites with improved biodegradability. In recent juncture, lignocellulosic fibers such as hemp, jute, kenaf and sisal fiber are extensively used as a substitute of a polymer in a polymer matrix for reducing the impact of polymer on the environment worldwide. Generally, cellulose (67-74 %), hemicellulose (16-22 %) and lignin (3.3-5.7 %) are found in a hemp fibre (Dayo et al., 2017; Zegaoui et al., 2018). Higher cellulosic content of hemp fiber has attained a lot of attraction of the researchers to substitute conventionally derived materials with natural fiber for various green applications. Due to strong stiffness and non-compatibility property of natural fiber, researchers often find it difficult to replace the non-biodegradable materials having strong mechanical strength, high thermal stability and hydrophobic quality for packaging applications. The hygroscopic nature of hemp fiber in a matrix weakens the bond between natural fiber and polymer. However, this behavior causes a high moisture absorption in composites and thus reduces the mechanical strength of a film. To overcome this problem, alkali-treated natural fiber was introduced in a polymer matrix (Islam et al., 2011; Stevulova et al., 2014; Suardana et al., 2011). This treatment eliminates the ester bonds between the Holocellulose and lignin and makes natural fiber more compatible in a matrix. The dire demand of green packaging film with outstanding thermal stability, better mechanical strength, desirable water vapor permeability, hydrophobicity, and biodegradability is thus fulfilled and it encourages the researchers to prepare an alkali treated-hemp fiber based polymeric composite film.

In the present work, hemp fiber is used as a strength enhancement agent in a polymer matrix to fabricate insulating materials, packaging films, and building materials. The effects of weight fraction of natural fiber in composites were also investigated. As an outcome, hemp fiber provided remarkable tensile strength in bio-composites (Dupeyre

and Vignon, 1998; Holbery and Houston, 2006; Jarabo et al., 2012). Many authors have made a serious attempt to use hemp fiber in a polymer matrix and visualized the significant impacts on mechanical & thermal characteristics. Some of the authors have also used coupling agent (maleic anhydride) for attaining a reliable adhesion between the polymer and hemp fiber (Etaati et al., 2014; Etaati et al., 2013; Grubeša et al., 2018; Khan et al., 2018; Madhusudhana et al., 2018; Sarasini et al., 2018; Wu et al., 2018). In this paper, the authors have examined the mechanical stiffness of alkali-modified hemp fiber based composites film and observed the remarkable effect on hydrophobicity and mechanical strength. Such composites have shown positive potential in mechanical strength in comparison to glass fiber reinforced composites (Vilaseca et al., 2018; Zegaoui et al., 2018). Many lignocellulosic materials such as rice straw, cotton stalk fibers, bagasse, sisal, jute, rice hulls, and wheat straw have been used in polyethylene, polypropylene, polylactic acid, polyvinyl alcohol matrix for packaging applications (Ayrilmis et al., 2013; Babaei et al., 2014; Haddar et al., 2018; Hou et al., 2014; HPS et al., 2017; Khalil et al., 2016; Orsuwan and Sothornvit, 2018; Perumal et al., 2018). In this study, the authors optimized the properties of natural fiber based PHBV packaging film using response surface methodology (Zhao et al., 2019). Bagheri et al., 2019 optimized the water migration, colour and mechanical characteristics of cellulose nanofiber based glutin/carboxymethyl cellulose film using RSM for packaging applications.

To carry out an optimization of the process, RSM is the best empirical design based on mathematical and statistical techniques according to our application (Bezerra et al., 2008). However, this empirical method is used to curtail the number of experiments and perform optimization of the process. RSM provides the simultaneous effects of different independent factors on various response factors for achieving the optimum output

variables (Mohamed et al., 2018). RSM is a technique that starts from an initial guess to the final optimized response. Some authors explored the suitability of CCD-RSM to obtain the most favourable values of independent factors and attained the optimized response in their studies (Abdulrahman Oyekanmi et al., 2019; Mohamed et al., 2018). It is a combination of mathematical and statistical approach that provides the appropriate set of experiments. After performing the predefined set of experiments, optimized output variables are investigated by CCD-RSM to examine the order of the system (Leardi, 2009).

This paper has emphasized the use of polyethylene and polypropylene along with treated hemp fiber for packaging applications. In this study, numerous appropriate set of experiments on the basis mass of PE, PP and alkali treated-HF were performed and the effect on different response variables (tensile strength, flexibility and WVTR) was observed. Moreover, a quadratic model was used to attain higher mechanical stability, moderate elongation limit and lower WVTR. Further, the optimized film was characterized using TGA, WVP, tensile testing, impact test, optical characteristics test and contact angle.

4.2 Materials & Methods

4.2.1 Packaging Materials

Hemp fiber was rendered by a farmer near IIT BHU, Varanasi, Uttar Pradesh (India). Initially, primary impurities of Hemp fiber were removed using distilled water and placed in an oven for 8 hours at a temperature of 80˚C. Further, hemp fiber was ground and passed through an 80-120 mesh screen size. Hemp fiber is passed through 80 mesh screen and retained by 120 mesh screens. So, the average particle size of the hemp fiber taken for further experiments was in between 0.177 to 0.125 mm. Polymers (LR grade)

were purchased from Sigma Aldrich (USA), and required solvent xylene, sodium hydroxide were procured from Fisher Scientific (USA).

4.2.2 Alkali treatment of hemp fiber

Treatment of natural fiber is one of the most admirable techniques to make biomass more compatible with polymer adhesion. This process can be accomplished using various chemicals like acid, alkali, salts, oxidants and solvent. In this present study, hemp fiber was subjected to alkali treatment. In alkali treatment, 5 g sieved hemp fiber was treated with 100 ml NaOH (1%, 3%,5%,7%, 10%) at 60˚C for one hour. The undesired liquid was drained using a vacuum pump filtration technique. The biomass was placed in an oven at 80˚C for 8 hours (Mussatto, 2016).

4.2.3 Compositional analysis

To study the percentage removal of hemicellulose and lignin from agro-waste, the compositional analysis of agro-waste was performed. Holocellulose, hemicellulose, cellulose and lignin contents of agro-waste and alkali treated-agro-waste were calculated (Bledzki et al., 2010).

4.2.3.1 Lignin contents

In this section, 2 g of agro-waste was treated with 15 ml of 72% H_2SO_4 at a temperature of 25 ^{O}C. The mixture was continuously stirred for two and a half hours. Further, 200 ml of distilled water was mixed in the mixture and heated for the next two hours. After 24 hours, the mixture was washed with distilled water until it attained pH 7. The washed solution was dried in an oven at a temperature of 80°C for 8 hours and cooled down in desiccator. The dried lignin material was weighed (Bledzki et al., 2010).

4.2.3.2 Holocellulose contents

To determine the holocellulose, 3 g of dried agro-waste was treated with 0.5 g of glacial acetic acid, 160 ml of distilled water, and 1.5 g of NaCl in a conical flask which was placed in a water bath at a temperature of 75°C for an hour. Subsequently, the same amounts of acetic acid and NaCl were added three times hourly. The resultant solution was placed in an ice bath for 8 hours. The Holocellulose content was separated from the mixture through filtration and washed with acetone, ethanol and distilled water to make acid free material. Holocellulose content was dried in an oven at a temperature of 80°C for 8 hours (Bledzki et al., 2010).

4.2.3.3 Cellulose contents

2 g of holocellulose was treated with 10 ml of 17.5% NaOH at a temperature of 20°C with continuous stirring using a glass rod. Further, 10 ml NaOH was added in the solution repeatedly every 5 min for half an hour. After that, 33 ml of distilled water was added to the solution and kept it for another half an hour. The residue was filtered using a filtration unit and washed with 100 ml of 8.3% NaOH and 200 ml of distilled water. After that, the water-washed residue was again washed with 15 ml of 10% acetic acid and 200 ml of distilled water. The washed cellulose was dried and weighed (Bledzki et al., 2010).

4.2.3.4 Hemicellulose contents

The subtraction of cellulose content from holocellulose content was hemicellulose content present in the agro-waste (Bledzki et al., 2010).

4.2.4 Preparation of polyethylene/polypropylene/alkali treated-hemp fiber film

Biocomposite film at different compositions of polyethylene, polypropylene and alkali treated-HF were prepared using solution casting method. Initially, polyethylene and polypropylene were dispersed in xylene at 130˚C for an hour. Further, alkali treated-HF was blended in the solution and mechanically stirred for half an hour at 600 rpm. Subsequently, the synthesized solution was cast in a petri dish for drying. After drying, the films were wrapped using aluminium foil for restricting the further uptake of moisture from the surroundings.

4.2.5 Experimental design and optimization for polyethylene/polypropylene/alkali treated- hemp fiber based biocomposite film

In an empirical design, RSM was selected to acquire the optimized parameters for the fabrication of PE/PP/alkali treated-hemp fiber composite. CCD-RSM is representing the combination of both mathematical and statistical design tools that provide optimized response variables. Moreover, this design has a lot of benefits as compared to traditional methods such as it requires less time to perform, provides significant interaction between independent factors and responses, and minimization of cost. CCD is also applied to enhance the correctness of the experiments. In addition, CCD is generally offered central points and axial points factors. The idea of repeating the central points in CCD technique is just maintaining the reliability of the experiments (Dixit and Yadav, 2019b).

RSM is chosen to achieve higher mechanical strength, moderate elongation limit and lower WVTR in order to prepare a film for packaging applications. The amounts of PE,

PP and alkali treated – HF were chosen as process variables and the ranges of amounts of PE, PP and alkali treated – HF were 1.08-1.8g, 0.72-1.2 g, and 0-1.2g, respectively. Twenty experiments (N) need to be carried out in this model as derived from equation 1 in which a number of process factor was three, factorial points(2^n) was eight, axial points (2n) was six and replicates at center points (n_c) was three.

$$N = 2^n + 2n + n_c \quad (1)$$

Stat-Ease design software (version -11) was used to apply CCD-RSM technique for optimization of biocomposite film (Tables 4.1 & 4.2). In this study, the actual value for responses was near to the predicted value of responses. Moreover, this behaviour is exhibiting the accuracy of the CCD model. Moreover, TS exhibits the mechanical stability, EAB signifies flexibility and WVTR explores transmission rate for water vapor through the film. In addition, the second order polynomial equation is chosen for optimization of the process. The general mathematical second order polynomial equation is represented as.

$$Y = b_0 + \sum_{i=1}^{k} b_i X_i + \sum_{i=1}^{k} b_{ij} X_i^2 + \sum_{i_{i>j}}^{k} \sum_{j}^{k} b_{ij} X_i X_j + \varepsilon \quad (2)$$

Where i shows the linear coefficient, k shows the number of parameters used in this study, j shows the quadratic coefficients, b_0 shows the regression coefficient, and ε shows the random error.

Table 4.1 Variables used in the experimental design represented with actual and coded values.

Variables	Symbol	Coded level		
		-1	**0**	**+1**
Polyethylene	PE	1.08 g (25.71%)	1.44 g (34.28%)	1.8g (42.85%)
Polypropylene	PP	0.72 g (17.14%)	0 g (22.85%)	1.2 g (28.51%)
Alkali-treated-hemp fiber	Alkali-treated-HF	0	0.6 g (14.28%)	1.2 g (28.51%)

Table 4.2 Experimental design matrix for PE/PP/alkali treated-HF composite film with responses.

Run	A:Polyethylene	B:Polypropylene	C:Alkali treated-HF	Tensile strength (MPa)		Elongation at break (%)		WVTR ($g.m^{-2}.day^{-1}$)	
				Actual Value	**Predicted Value**	**Actual Value**	**Predicted Value**	**Actual Value**	**Predicted Value**
1	0	0	0	46.25	45.23	122.21	122.38	55.23	56.59
2	-1	+1	+1	47.00	46.72	118.12	118.16	6+17	61.59
3	-1	+1	-1	34.00	34.63	125.00	125.05	56.70	56.67
4	0	0	0	45.00	45.23	122.10	122.38	56.59	56.59
5	0	0	0	44.75	45.23	122.50	122.38	57.62	56.59
6	-1	-1	+1	41.91	42.30	119.50	119.47	68.10	67.60
7	0	+1	0	43.65	43.01	121.11	121.04	55.00	54.51
8	0	0	0	45.67	45.23	122.75	122.38	57.23	56.59
9	+1	0	0	47.69	48.16	123.00	123.15	53.00	53.31
10	0	0	-1	38.61	39.58	126.25	126.22	54.25	54.30
11	+1	-1	+1	47.35	46.52	120.31	120.24	57.00	56.91
12	0	0	0	46.12	45.23	122.75	122.38	57.88	56.59
13	-1	-1	-1	29.31	28.23	124.68	124.70	57.50	57.54
14	0	-1	0	37.69	39.14	121.31	121.44	57.50	58.48
15	0	0	0	45.23	45.23	122.12	122.38	55.99	56.59
16	0	0	+1	50.00	49.84	120.00	120.09	58.00	58.44
17	-1	0	0	42.31	42.65	122.31	122.22	61.00	61.18
18	+1	+1	-1	42.00	41.41	126.12	126.13	51.25	51.63
19	+1	-1	-1	38.00	38.08	125.69	125.63	54.00	53.56
20	+1	+1	+1	47.00	47.88	119.12	119.08	50.00	49.84

Analysis of variance (ANOVA) was chosen to exhibit the interaction values of independent factors and output variables according to the suggested model. This ANOVA analysis examines the appropriateness of the second order polynomial equation in terms of numerous design elements such as determination coefficient (R^2), p-value, F value, adjusted determination of coefficient (R^2_{adj}), and degree of freedom (DF) in order to observe the correctness of the suggested model. Moreover, the value of p is less than 0.05 signifies suitability of the model. The graphical plots provided by the CCD model illustrate the discrete and combined influences of the process factors on TS, EAB and water vapor transmission rate for alkali treated-hemp fiber reinforced polyethylene/polypropylene composite.

4.2.6 Characterization of native and pre-treated-hemp fiber

4.2.6.1 XRD analysis

The crystalline changes in native-HF and alkali treated-HF were studied using X-ray diffractometer (XRD, model mini flux II, Rigaku, Japan) with a scanning rate of 5° per minute in the range of 0° to 70° (2θ) along with wavelength 1.54060 A^o.

4.2.6.2 FTIR analysis

To study the functional groups, present in biomass, FTIR analysis of native-HF and alkali treated-HF was recorded using Thermo-Nicolet 5700 (Waltham, United States) technique in transmittance mode. FTIR spectra were obtained in a range of 4000-400 cm^{-1} wavenumber in this analysis with a resolution of 4 cm^{-1}.

4.2.6.3 Compositional analysis

To study the percentage removal of hemicellulose and lignin from agro-waste, the compositional analysis of agro-waste was performed. Holocellulose, hemicellulose, cellulose and lignin contents of agro-waste and alkali treated-agro-waste were calculated (Bledzki et al., 2010).

4.2.6.4 SEM analysis

The surface morphology analysis of native-HF and alkali treated-HF was studied using scanning electron microscopy (SEM, model JEOL JSM5410, Japan). A gold coating was done on a polymeric composite sample to make our sample conductive for further analysis with an accelerating voltage of 20KV.

4.2.7 Characterization of polyethylene/polypropylene/alkali treated-wheat straw bio-composite film

4.2.7.1 SEM analysis

In this analysis, initially, NHF, alkali treated- HF, films were coated with gold alloy to make it conductive. The surfaces of NHF, alkali treated- HF and all prepared composite films were studied using ZEISS EVO – Scanning Electron Microscope, USA with 20 kV operating voltage.

4.2.7.2 FTIR analysis

FTIR spectra of all prepared composite films were obtained using Thermo Scientific iD7 ATR technique. Samples were analysed using transmittance mode from 400 to 4000 cm^{-1} wavelength with a 45° ZeSe crystal.

4.2.7.3 XRD analysis

To elucidate the crystalline changes, XRD analysis for PE/PP, PE/PP/NHF and PE/PP/alkali treated-HF were performed on The Rigaku mini II, Benchtop X-ray diffractometer (Japan) with a 1.54 A° wavelength of Copper- K_{α}. The scan range was in between 2 theta values of 10°- 70 ^{o}. The scan speed was set to 5°/min during the analysis.

4.2.7.4 TGA analysis

To visualize the changes in thermal stability for PE/PP, real PE packaging, PE/PP/NHF and PE/PP/alkali treated-HF films were investigated using the PerkinElmer instrument (USA). In this TGA analysis, the films were heated up to 700 ^{o}C from room temperature. Moreover, the heating rate was set to 10 ^{o}C/min under a nitrogen atmosphere.

4.2.7.5 Tensile test

Tensile strength, Flexibility, tensile modulus for PE/PP, real polyethylene packaging, real polyester packaging, PE/PP/NHF and PE/PP/alkali treated-HF (0.25±0.03 mm thickness) films were analyzed according to ASTM D0882 using INSTRON 5982 Floor Model Machine, USA. The testing speed was 3 mm/min.

4.2.7.6 Contact angle measurement

Hydrophobic property for PE/PP, real polyethylene packaging, real polyester packaging, PE/PP/NHF and PE/PP/alkali treated-HF films were investigated using contact angle measurement test. Initially, films were cleaned with ethanol and dried in a dryer at a temperature of 50°C for 8 hours. Further, drop shape analyser (DSA25 Series, Germany) was used to evaluate the contact angles for all prepared composite films using a sessile drop method.

4.2.7.7 Water vapor permeability

WVP for PE/PP, real polyethylene packaging, real polyester packaging, PE/PP/NHF and PE/PP/alkali treated-HF films was determined. In this test, a wet chamber (airtight) covered by the polymeric composite film is fabricated and measured its weight. Subsequently, a wet chamber is placed in an incubation chamber conditioned at fixed relative humidity and a constant temperature. The loss in the weight of the chamber is recorded regularly at a period of one day. Weight loss of a wet chamber fixed with

films indicates the water vapor transmitted through the film (Râpă et al., 2016; Sirviö et al., 2014). Water vapor transmission rate through films is calculated using equation.

$$WVTR = \frac{WC1 - WC2}{WC1 * A * day} \quad (3)$$

where WC1 is the initial weight of the wet chamber, WC2 is the final weight of the wet chamber and A is the exposed area of the wet chamber. In the present work, the test temperature was 23 ^{o}C and the relative humidity was maintained about 53%. Water vapor permeability is also calculated using the following equation.

$$WVPR = \frac{WVTR * T}{S(R1 - R2)} \quad (4)$$

where S represents a saturation vapor pressure at 23 ^{o}C (2800 Pa), R1 exhibits the relative humidity inside the wet chamber, R2 exhibits the relative humidity of incubation chamber, and T exhibits the thickness of the film (m).

4.2.7.8 Dart Impact test

Impact test for PE/PP, real polyethylene packaging, real polyester packaging, PE/PP/NHF and PE/PP/alkali treated-HF films was performed using Dart Impact tester (Asian Test Equipments, Hapur, India) with 2.93 m/s striking velocity according to ASTM D1709 free-falling dart impact method. The films were cut in the size of 220mm X 220mmX 0.25mm and dropped the dart of different weights (10 g to 100 g) from a height (43 cm) for calculating the impact strength.

$$\text{Impact energy } (KE) = \frac{1}{2}\, m\, v^2 \quad (5)$$

$$\text{Impact Force} = \frac{KE}{d} \quad (6)$$

4.2.7.9 Optical characteristics test

In this test, Elico SL 210 UV VIS spectrophotometer was used to study optical characteristics for PE/PP, real polyethylene packaging, real polyester packaging, PE/PP/NHF and PE/PP/alkali treated-HF films. In this analysis, a visible light transmission rate through films is recorded over the wavelength range (400-800 nm) using a vacant optical glass as a reference.

4.3 Results and discussion

4.3.1 Characterization of native-HF and alkali treated-HF

In this section, XRD analysis, FTIR analysis, compositional analysis and SEM analysis for NHF and alkali treated-HF have been presented.

4.3.1.1 XRD analysis

The crystalline changes in the hemp fiber after pre-treatment were analysed using XRD analytical technique and XRD graph is shown in Figure 4.1. The presence of orderly arranged H-bonds in cellulosic fibers causes the crystalline structure of hemp fiber. The major peak for alkali treated hemp fiber exhibited the cellulose crystalline area in fiber. The two major peaks for untreated and alkali treated-hemp fiber at different concentrations viz. 1%, 2.5%, 5%, 7.5%, 10% are at 16° and 22° 2 theta values. The peaks at 16° and 22° 2 theta represents (101), (202) planes, respectively which are exhibit cellulose I structure according to JCPDS. No. 03-0226.

The significant broader peak for wheat straw is found at 21.12° for native-HF, 21.58° for 1% NaOH treated-HF, 21.94° for 3% NaOH treated-HF, 21.95° for 5% NaOH treated-HF, 22.12° for 7% NaOH treated-HF, and 22.30° for 10% NaOH treated-HF, respectively. The % crystallinity for native-HF, 1% NaOH treated-HF, 3% NaOH treated-HF, 5% NaOH treated-HF, 7% NaOH treated-HF, and 10% NaOH treated-HF is

found to be 60.37, 62.98, 65.49, 69.21, 71.41, 70.11 respectively. Similar results at 22° 2-theta show enhanced cellulose peak in treated-HF as compared to native-HF.

An increase in peak height at 22° 2θ reveals successfully removal of lignin and hemicellulose from hemp fiber. Similar results have been explained by Pickering et al., 2011 in their published literature. Hence, alkali treatment decreases the water absorption of treated-hemp fibre for enhancing its suitability for polymer adhesion. The authors explained similar results in their published literature (Kalia and Vashistha, 2012). The higher peak height at 22° 2θ is correlated with higher mechanical strength of treated-hemp fiber (Alemdar and Sain, 2008).

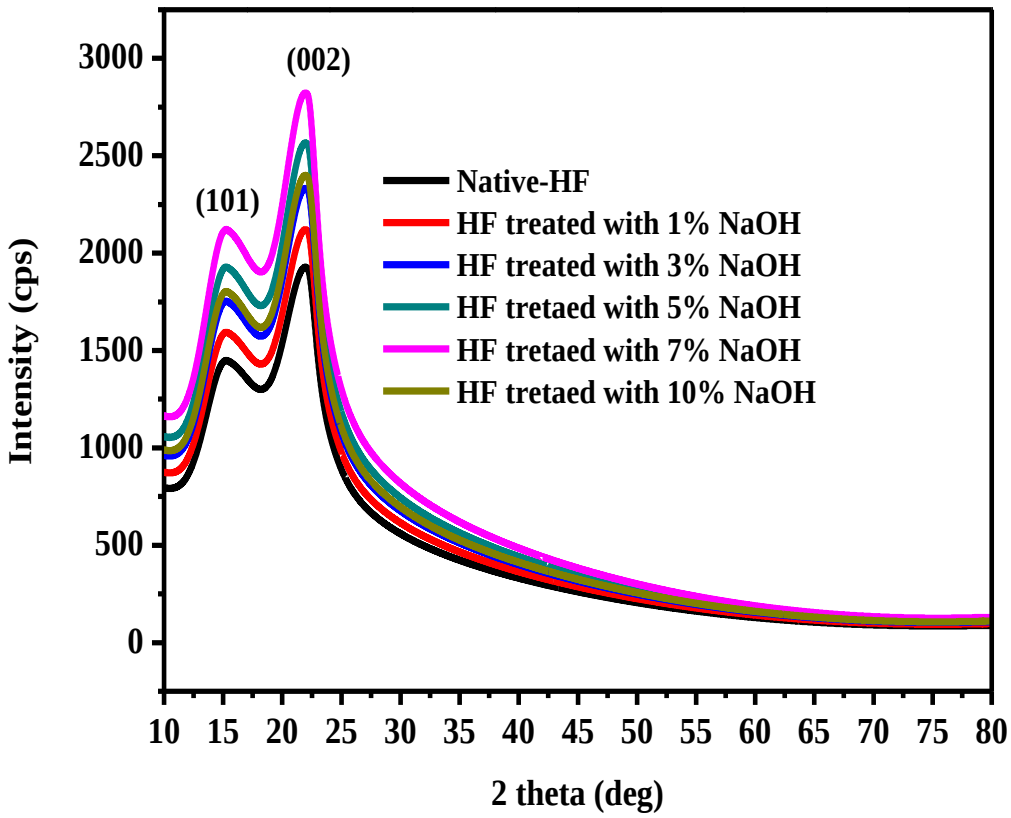

Figure 4.1 XRD analyses for native-HF and alkali treated- HF.

4.3.1.2 FTIR analysis

FTIR is an imperative technique for visualizing the information of different functional groups present in the hemp fiber. The structural variations in the hemp fiber after NaOH treatment were analysed using FTIR analytical method in 3500-600 cm^{-1} wavelength range. The impact of various concentrations of NaOH viz., 1%, 2.5%, 5%, 7.5%, 10% on hemp fiber has been depicted in Figure 4.2.

Peak at 1550-1610 cm^{-1} corresponds to carboxylic functional group or hemicellulose present in the biomass (Tang et al., 2015). Therefore, that peak decreases after pre-treatment with higher concentration of NaOH showing degradation of hemicellulose in the treated-biomass. Peak at 1220-1260 cm^{-1} represents the acetyl function group existing in the hemp fiber. Peak at 1400-1500 cm^{-1} represents lignin present in biomass that is also decreasing in FTIR spectra of treated-HF (Laadila et al., 2017). C-H stretching corresponding to peak at 2850-3000 cm^{-1}confirms cellulose present in the hemp fiber. This peak appears more effective after pre-treatment revealing the significant decrement in percentage of hemicellulose and lignin in the treated-hemp fiber. This result shows similarity with the published article (Cao and Tan, 2004). Peak at 2900-3400 cm^{-1} assigned to hydroxyl groups in biomass is continuously decreasing at higher concentrations of NaOH treatment revealing the reduction of hydroxyl groups. This depicts the effectiveness of alkali treatment on hemp fiber and resulting improvement in the moisture resistance characteristics of treated-hemp fiber.

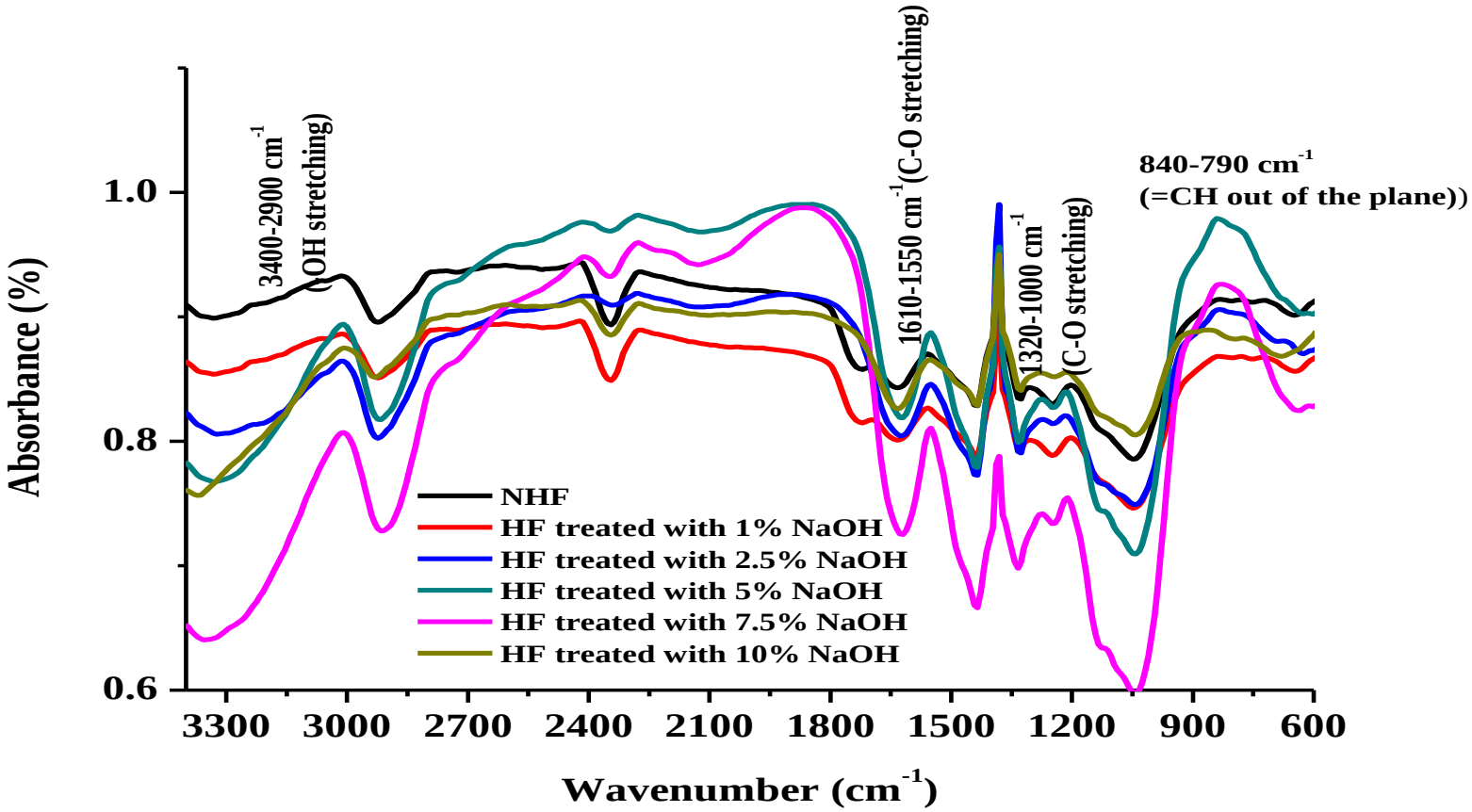

Figure 4.2 FTIR analyses for native-HF and alkali treated- HF.

4.3.1.3 Compositional analysis

Compositional analysis of native-agro-waste and NaOH treated- agro-waste is depicted in Table 4.3. Generally, hemicellulose exhibits xylose, mannose and arabinose contents present in the biomass. Lignin is an insoluble resin material of phenolic characteristics. Holocellulose content is a summation of hemicellulose and cellulose present in the biomass (Bledzki et al., 2010).

After alkali treatment, hemicellulose and lignin contents get reduced from 16 % to 8.09% and 8 % to 0.19 % in hemp fiber. This exhibits the enhancement of desirable cellulose percentage in hemp fiber. But for NaOH concentration higher than 7%, removal of cellulose from hemp fiber occurs. So, treatment of hemp fiber with 7% NaOH is optimum for cellulose recovery and shows better results for reinforcement applications (Agbor et al., 2011).

Table 4.3 Compositional analyses for native-HF and alkali treated-HF.

Agro-waste	**Lignin (%)**	**Holocellulose (%)**	**Hemicellulose (%)**	**Cellulose (%)**
Native-HF	8	77	16	61
HF treated with 1% NaOH	4.16	80.84	12.56	68.28
HF treated with 3% NaOH	2.56	82.48	10.40	72.08
HF treated with 5% NaOH	0.96	84.04	9.76	74.28
HF treated with 7% NaOH	0.19	84.81	8.09	76.72
HF treated with 10% NaOH	1.28	83.72	10.17	73.55

4.3.1.4 SEM analysis

SEM analysis was used to elucidate the surface modification in hemp fiber after alkali treatment. The surface images of NHF and alkali treated-HF are shown in Figure 4.3 with a magnification of 2.00 kx with 20.0 kV voltage. No void openings are found at the surface of NHF (Figure 4.3(a)). The SEM image has explored the existence of a rough surface with an excess amount of impurities such as lignin, wax and pectin present in the NHF. Moreover, after alkali treatment, SEM image is showing a rough surface with porous structures at the surface of treated-HF (Figure 4.3(b)).

Rough surface of NHF with many impurities shows similarty with the results reported in previous studies (Asumani et al., 2012; Lee et al., 2013). The surface is rough with some void openings representing a removal of lignin and hemicellulose from the HF. The existance of some void openings at the surface confirms the destruction of the external wall of HF. SEM images of treated-HF shows suitability of fiber for polymer adhesion. Luo et al., 2014 prepared treated-corn fiber/polylactic composites and stated equivalent outcomes in their published literature.

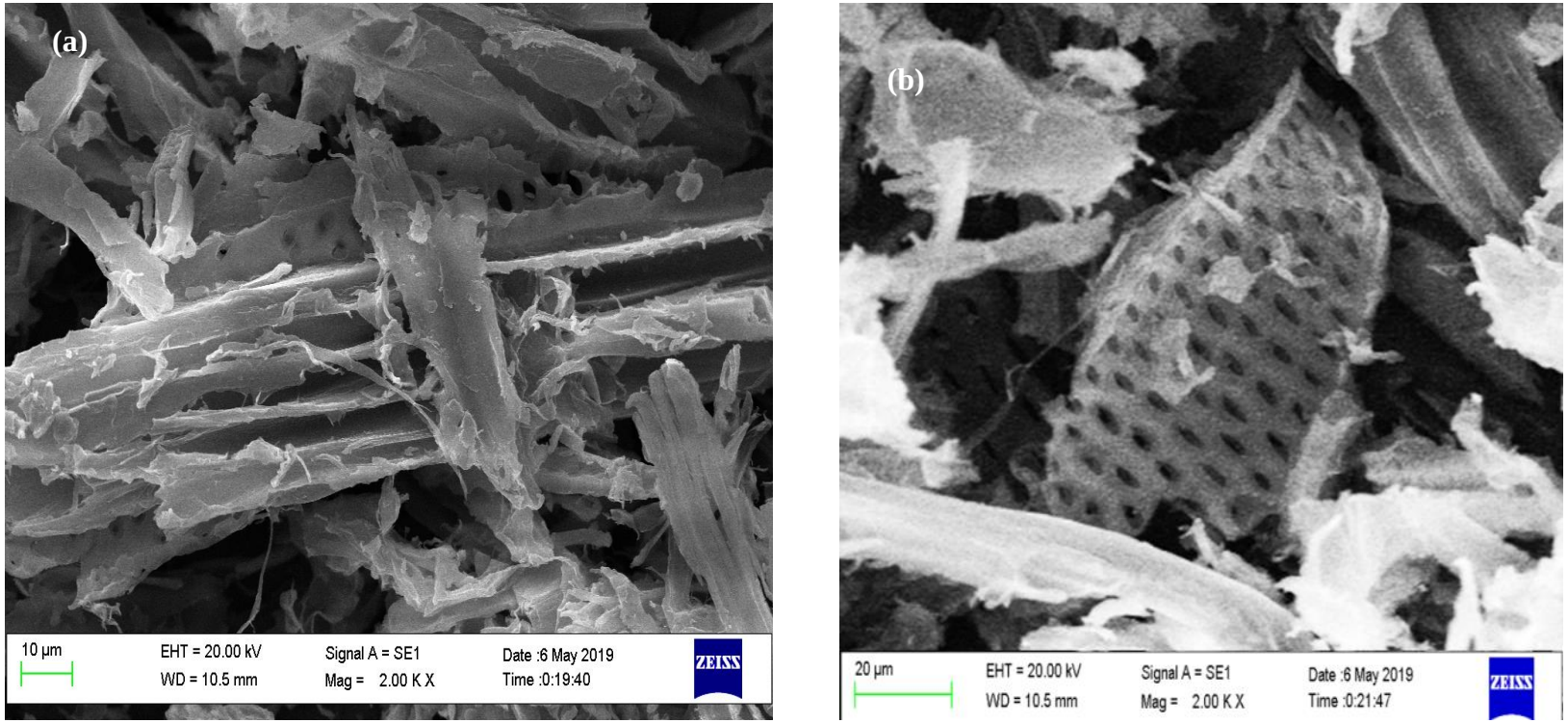

Figure 4.3 SEM analyses for native-wheat straw and alkali treated- hemp fiber (a) NHF (b) Alkali treated-HF.

4.3.2 RSM and ANOVA analysis

4.3.2.1 ANOVA and RSM analysis for tensile strength, Elongation at break and WVTR of PE/PP/Alkali treated-HF biocomposite film

4.3.2.1.1 Data adequacy check of the Model

Figure 4.4 represents the actual and the predicted values of TS, EAB and WVTR. The actual values are response data obtained from experimental run and the predicted values are originated from RSM model. Both values are very closer to each other representing the suitability of the suggested model. Lu et al., 2009 explained the equivalent results in their published article. The reasonable R^2 values 0.9808 for TS, 0.9948 for EAB and 0.9731 for WVTR show the suitability of RSM predicting the values of responses. Equivalent outcomes are reported by authors in their published articles (Satapathy and Das, 2014).

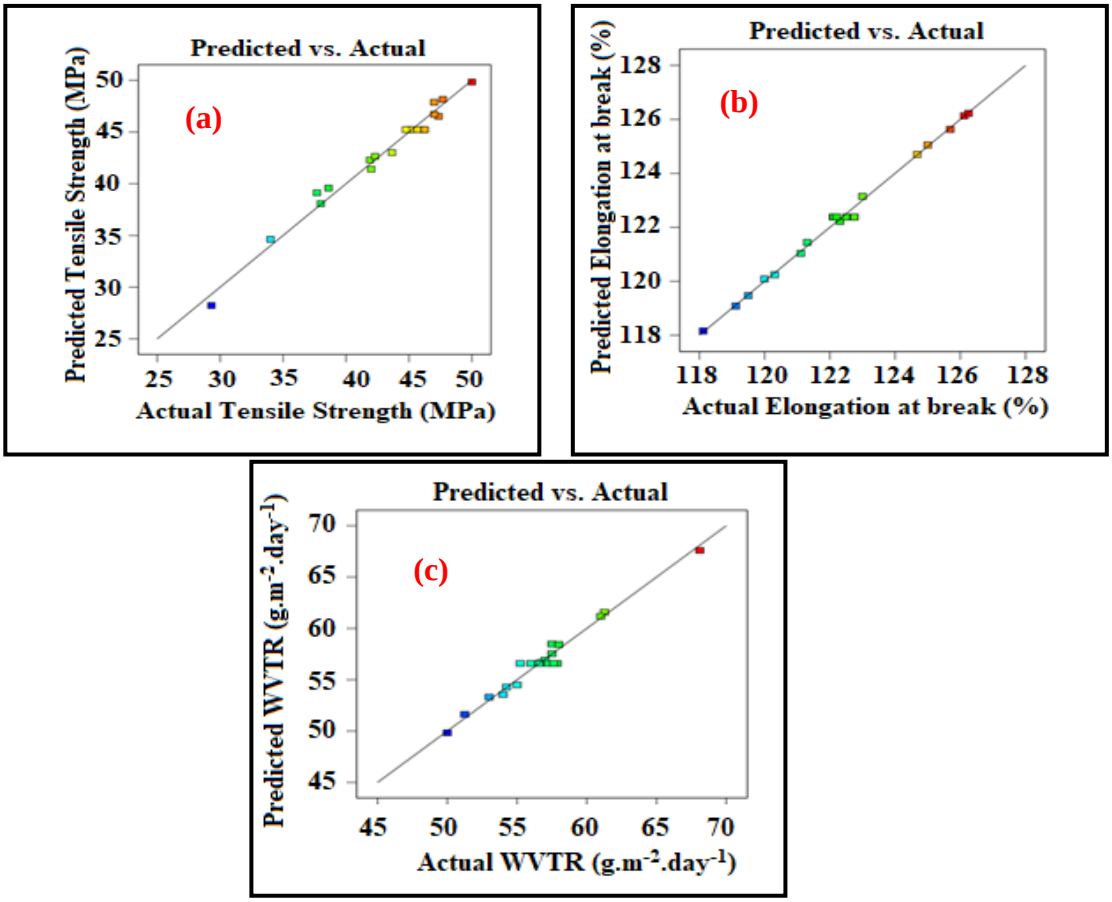

Figure 4.4 Relationship between actual and predicted values of model for the prepared composites involving HF (a) Tensile strength and (b) Elongation at break (%) (c) Water vapor transmission rate.

4.3.2.1.2 Effect of process variables on Tensile strength

The suggested polynomial equation for TS of the film is depicted by the equation.

$$Y_{TS} = +45.23+2.75A +1.94B +5.13C -0.7663AB -1.41AC -0.4938BC +0.1705A^2 - 4.16B^2 -0.5245C^2 \quad (7)$$

Table 4.4 depicts effective p and f values prove the reliability of the ANOVA analysed suggested model (f= 56.86, p<0.0001). The p and f factors can also be used to check the suitability of the linear terms (A, B, C), interaction terms (AB, BC, AC) and quadratic terms (A^2, B^2, C^2) of the model. The significant p-values for A, B, C, AC, B^2 are <0.0001, <0.0001, <0.0001, 0.0024, <0.0001, respectively. The standard deviation is 0.9841, and difference between R^2 predicted tensile strength and R^2 adjusted tensile strength is less than 0.2. These concluded outcomes represent the suitability of CCD-RSM model.

Three dimensional (3D) plots represent the dependability of TS with different process factors (Figure 4.5). At low and high concentrations of PP, TS increases up to higher value with surging the PE concentration from 1.08 g to 1.8 g (Figure 4.5 (a)). This demonstrated the benchmark impact of PE on TS. Analogous trends are observed in the graphical plots for variation in TS with different combinations of process factors (PE and alkali treated-HF, and PP and alkali treated –HF) for the film (Figures 4.5(c) and 4.5(e)). Moreover, this behaviour is enabling the use of alkali treated-HF in the fabrication of mechanically stable packaging film.

Table 4.4 ANOVA analysis for the tensile strength of PE/PP/alkali treated-HF from CCD. model.

Source	Sum of Squares	df	Mean Square	F-value	p-value	
Model	495.66	9	55.07	56.86	< 0.0001	**significant**
A-Polyethylene	75.68	1	75.68	78.14	< 0.0001	
B-Polypropylene	37.60	1	37.60	38.82	< 0.0001	
C-Alkali treated-HF	263.58	1	263.58	272.15	< 0.0001	
AB	4.70	1	4.70	4.85	0.0522	
AC	15.82	1	15.82	16.33	0.0024	
BC	1.95	1	1.95	2.01	0.1863	
A^2	0.0799	1	0.0799	0.0825	0.7798	
B^2	47.58	1	47.58	49.13	< 0.0001	
C^2	0.7567	1	0.7567	0.7813	0.3975	
Residual	9.68	10	0.9685			
Lack of Fit	7.82	5	1.56	4.20	0.0705	**not significant**
Cor Total	505.34	19				
Std. Dev.	0.9841	**R^2**	0.9808			
Mean	42.98	**Adjusted R^2**	0.9636			
C.V. %	2.29	**Predicted R^2**	0.7986			
		Adeq Precision	31.0591			

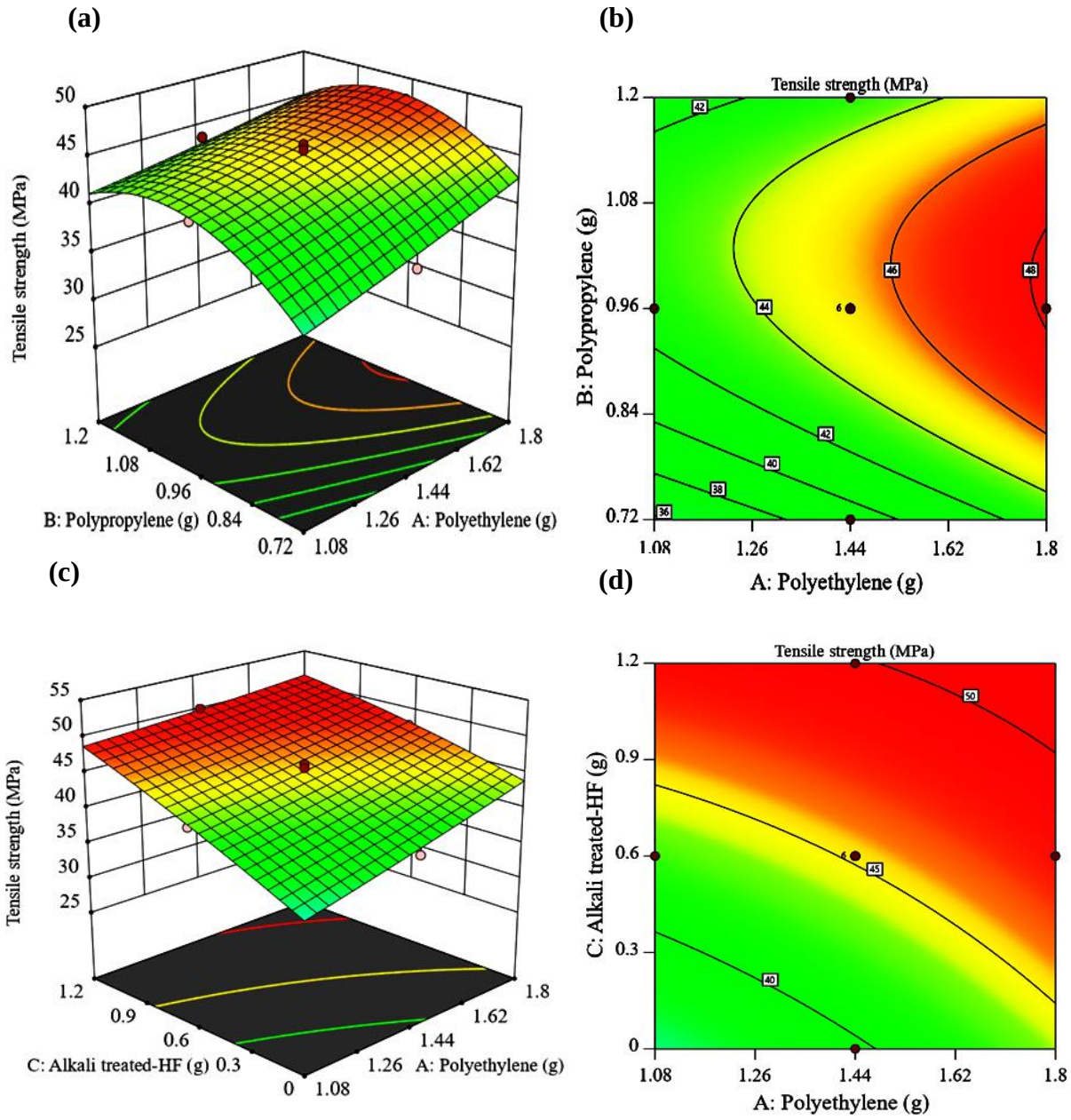
(a)
Tensile strength (MPa)
50
45
40
35
30
25
1.2
1.08
0.96
B: Polypropylene (g) 0.84
0.72
1.08
1.26
1.44
1.62
1.8
A: Polyethylene (g)
(b)
Tensile strength (MPa)
B: Polypropylene (g)
1.2
1.08
0.96
0.84
0.72
42
44
46
48
42
40
38
36
1.08
1.26
1.44
1.62
1.8
A: Polyethylene (g)
(c)
Tensile strength (MPa)
55
50
45
40
35
30
25
1.2
0.9
0.6
C: Alkali treated-HF (g) 0.3
0
1.08
1.26
1.44
1.62
1.8
A: Polyethylene (g)
(d)
Tensile strength (MPa)
C: Alkali treated-HF (g)
1.2
0.9
0.6
0.3
0
50
45
40
1.08
1.26
1.44
1.62
1.8
A: Polyethylene (g)

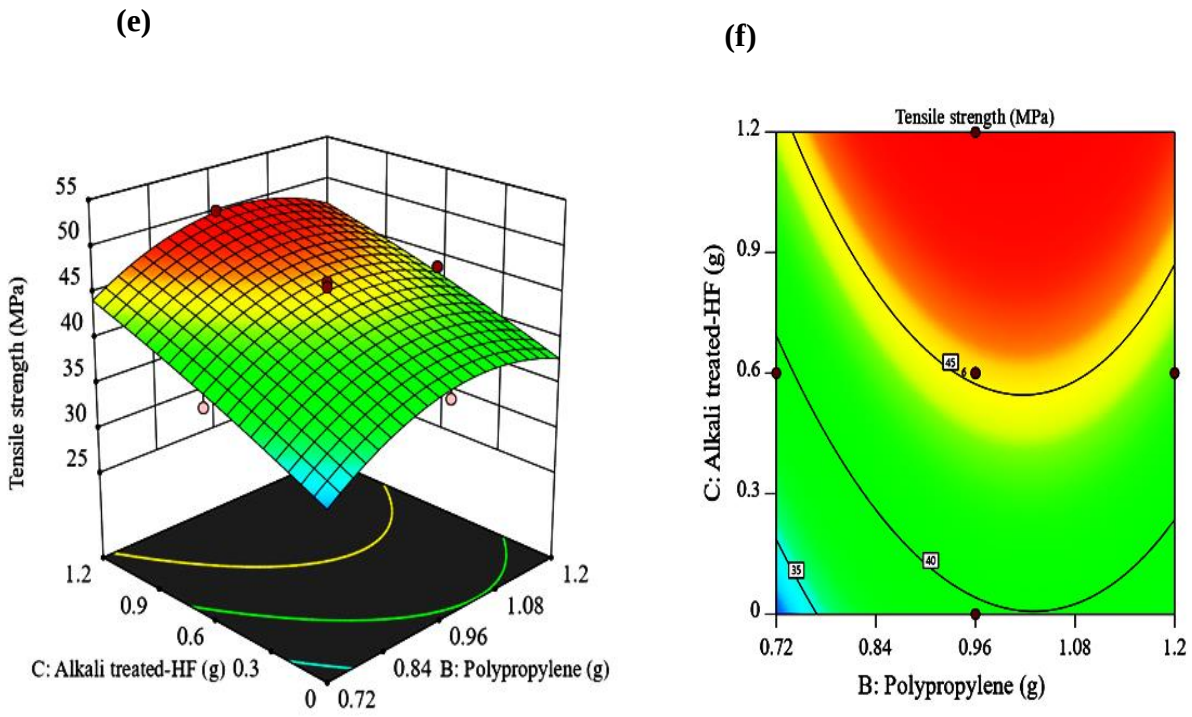

Figure 4.5 Three-dimensional response surface and contour plots of tensile strength showing the effect of (a) and (b) polypropylene and polyethylene; (c) and (d) alkali treated-HF and polyethylene; (e) and (f) alkali treated-HF and polypropylene.

4.3.2.1.3 Effect of process variables on Elongation at break (%)

The suggested model for EAB (%) of biocomposite film is as per the following equation.

$$Y_{EAB} = +122.38+0.4630A -0.2020B -3.07C +0.0375AB -0.0400AC -0.4150BC +0.3000A^2 -1.15B^2 +0.7700 C^2 \quad (8)$$

Table 4.5 shows reliable p and f values for quadratic model that are with in flexible limit (p value<0.0001, f value = 211.33). The individual significant p values for A, C, BC, B^2, C^2 are <0.0001, <0.0001, 0.0005, <0.0001, 0.0003 respectively, and minor difference between the predicted elongation R^2 value and adjusted elongation R^2 value assuring the suitability of RSM model.

Figure 4.6 demonstrates the reliability of EAB with process factors of film. Figure 4.6(a) represents that at low and high concentrations of PP, no substantial impact at constant concentration of PE. The similar pattern is shown in 3-D plot for variation in response EAB with PE and alkali treated-HF process factors (Figure 4.6(c)). Reduction in the flexibility of biocomposite film is observed with surging the concentration of alkali treated-HF from 0 to 1.2 g in Figure 4.6(e). Thus, it can be said that certain decrement is observed after addition of biomass and PP in the biocomposite film.

Table 4.5 ANOVA analysis for elongation at break (%) of PE/PP/alkali treated-HF from CCD model.

Source	Sum of Squares	df	Mean Square	F-value	p-value	
Model	102.15	9	11.35	211.33	< 0.0001	significant
A-Polyethylene	2.14	1	2.14	39.92	< 0.0001	
B-Polypropylene	0.4080	1	0.4080	7.60	0.0203	
C-Alkali treated-HF	94.19	1	94.19	1753.76	< 0.0001	
AB	0.0112	1	0.0112	0.2095	0.6570	
AC	0.0128	1	0.0128	0.2383	0.6359	
BC	1.38	1	1.38	25.65	0.0005	
A^2	0.2475	1	0.2475	4.61	0.0574	
B^2	3.61	1	3.61	67.13	< 0.0001	
C^2	1.63	1	1.63	30.36	0.0003	
Residual	0.5371	10	0.0537			
Lack of Fit	0.0777	5	0.0155	0.1692	0.9632	not significant
Pure Error	0.4594	5	0.0919			
Cor Total	102.68	19				
Std. Dev.	0.2317		**R^2**	0.9948		
Mean	122.35		**Adjusted R^2**	0.9901		
C.V. %	0.1894		**Predicted R^2**	0.9885		
			Adeq Precision	49.1887		

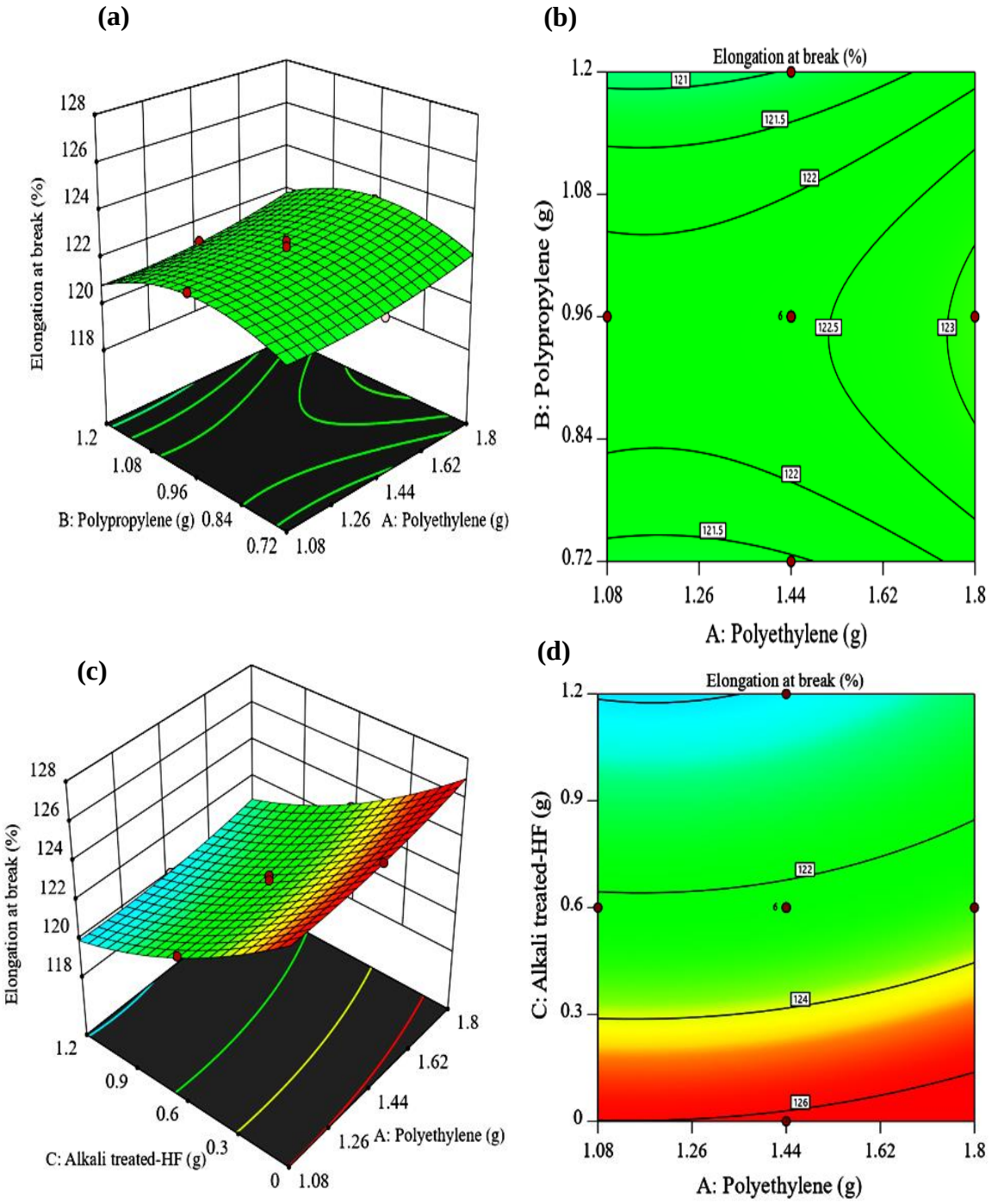
(a)
Elongation at break (%)
128
126
124
122
120
118
1.2
1.08
0.96
0.84
0.72
B: Polypropylene (g)
1.08
1.26
1.44
1.62
1.8
A: Polyethylene (g)
(b)
Elongation at break (%)
B: Polypropylene (g)
A: Polyethylene (g)
121
121.5
122
122.5
123
(c)
Elongation at break (%)
C: Alkali treated-HF (g)
A: Polyethylene (g)
(d)
Elongation at break (%)
C: Alkali treated-HF (g)
A: Polyethylene (g)
122
124
126

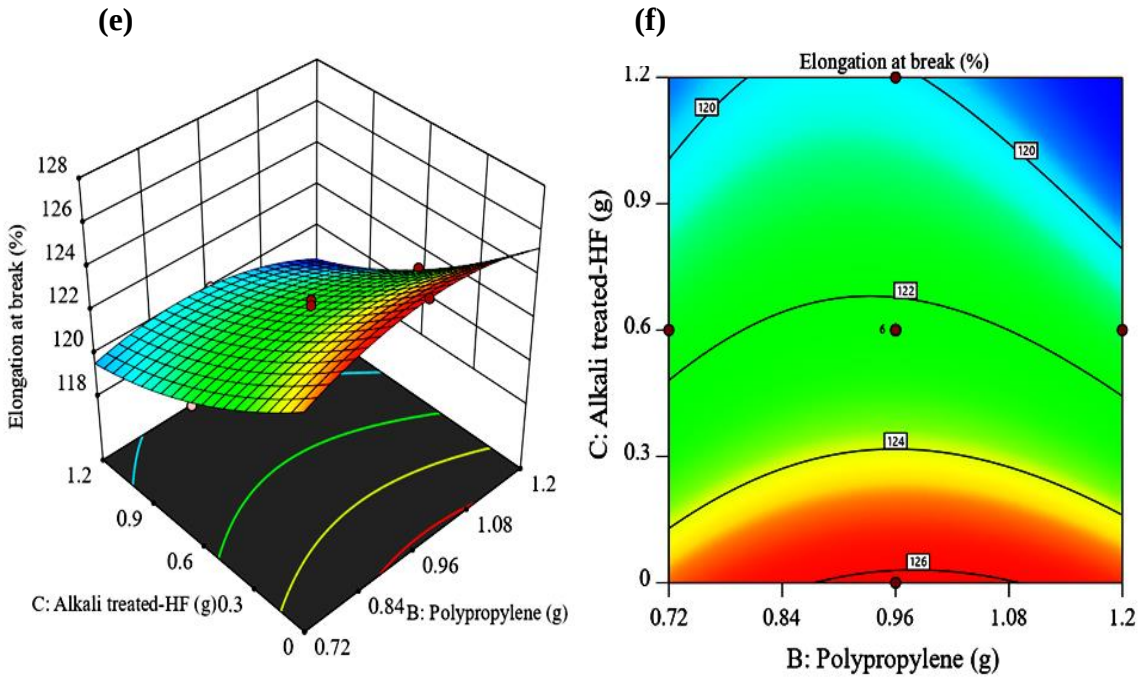

Figure 4.6 Three-dimensional response surface and contour plots of elongation at break showing the effect of (a) and (b) polypropylene and polyethylene; (c) and (d) alkali treated-HF and polyethylene; (e) and (f) alkali treated-HF and polypropylene.

4.3.2.1.4 Effect of process variables on WVTR

An empirical equation suggested by RSM which optimizes the process factors for WVTR of biocomposite film is as follows:

$$Y_{WVTR} = +56.59-3.93A -1.99B +2.07C -0.2650AB -1.68AC -1.28BC +0.6491A^2 - 0.1009B^2 - 0.2259 C^2 \quad (9)$$

The significant F value 40.21 with reliable p value <0.0001 suggests the satisfactory applications of CCD-RSM model for water vapor transmission rate. For all process variables (A, B, C, AC, BC) the p-value is less than 0.05. Moreover, this individual significant p-value and minor difference in between $R^2_{predicted}$ and $R^2_{adjusted}$ values assures reliable influence of process variables on water vapor transmission rate of film (Table 4.6).

3-D response plots for WVTR have been depicted in Figure 4.7. A significant decrement is found in the interaction pattern of PE and PP (Figure 4.7a)). Figures 4.7(c) and 4.7(e) explore similar trends for changes in the transmission rate of water vapor for packaging film with PE and alkali treated-HF process factors, and PP and alkali treated-HF process factors. These results are in favour of increasing the role of biodegradable alkali treated-HF in packaging film for obtaining the desirable water vapor migration rate.

Table 4.6 ANOVA analysis for water vapor transmission rate of PE/PP/alkali treated-HF from CCD model.

Source	Sum of Squares	df	Mean Square	F-value	p-value	
Model	274.41	9	30.49	40.21	< 0.0001	significant
A-Polyethylene	154.61	1	154.61	203.91	< 0.0001	
B-Polypropylene	39.52	1	39.52	52.12	< 0.0001	
C-Alkali treated-HF	42.72	1	42.72	56.35	< 0.0001	
AB	0.5618	1	0.5618	0.7409	0.4095	
AC	22.51	1	22.51	29.69	0.0003	
BC	13.21	1	13.21	17.42	0.0019	
A^2	1.16	1	1.16	1.53	0.2446	
B^2	0.0280	1	0.0280	0.0369	0.8515	
C^2	0.1403	1	0.1403	0.1851	0.6762	
Residual	7.58	10	0.7582			
Lack of Fit	2.40	5	0.4809	0.4644	0.7901	not significant
Pure Error	5.18	5	1.04			
Cor Total	282.00	19				
Std. Dev.	0.8708			**R^2**	0.9731	
Mean	56.76			**Adjusted R^2**	0.9489	
C.V. %	1.53			**Predicted R^2**	0.8952	
				Adeq Precision	28.8524	

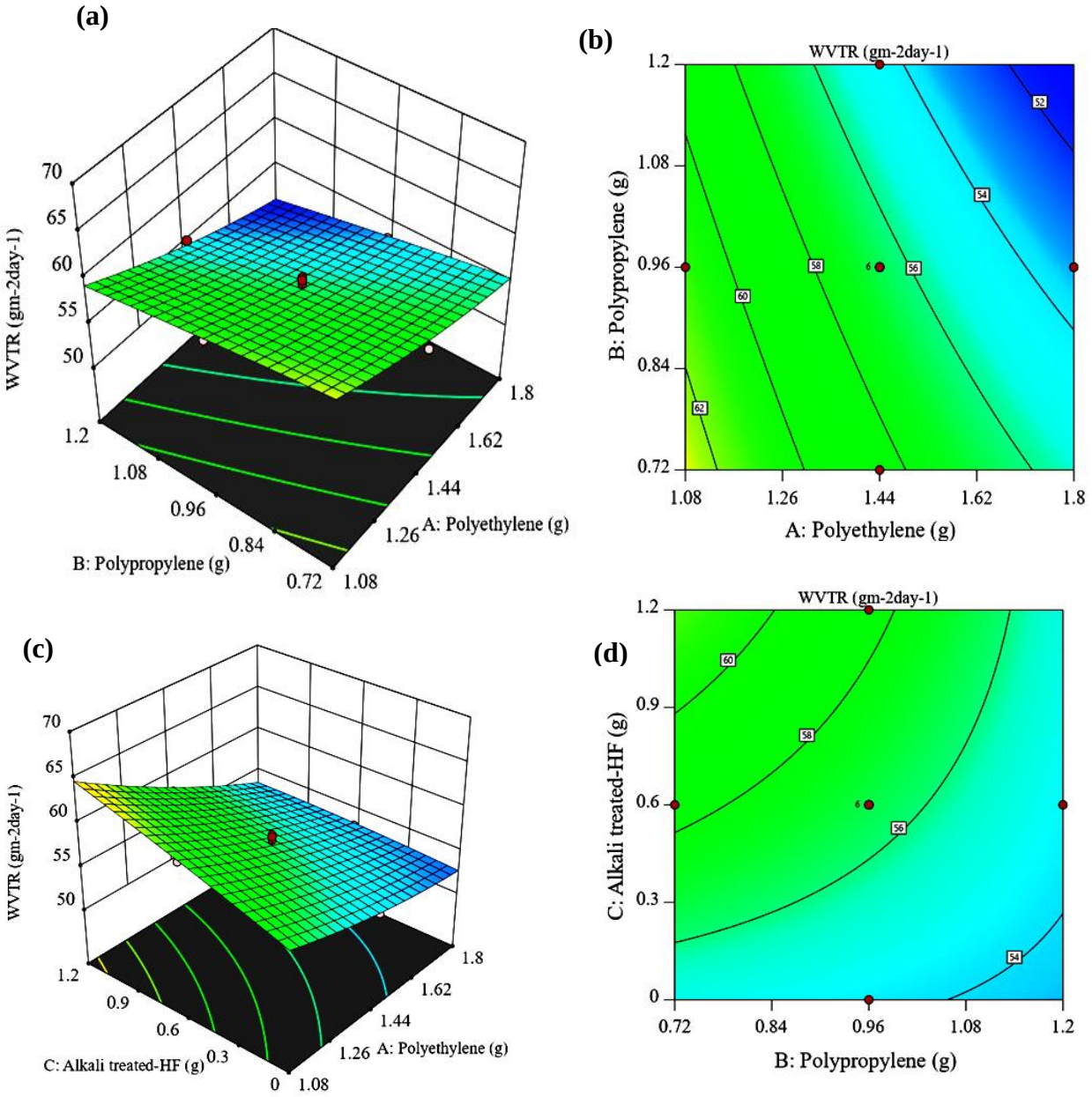
(a)
WVTR (gm-2day-1)
70
65
60
55
50
1.2
1.08
0.96
0.84
0.72
B: Polypropylene (g)
1.08
1.26
1.44
1.62
1.8
A: Polyethylene (g)
(b)
WVTR (gm-2day-1)
B: Polypropylene (g)
A: Polyethylene (g)
1.2
1.08
0.96
0.84
0.72
1.08
1.26
1.44
1.62
1.8
52
54
56
58
60
62
(c)
WVTR (gm-2day-1)
70
65
60
55
50
1.2
0.9
0.6
0.3
0
C: Alkali treated-HF (g)
1.08
1.26
1.44
1.62
1.8
A: Polyethylene (g)
(d)
WVTR (gm-2day-1)
C: Alkali treated-HF (g)
B: Polypropylene (g)
1.2
0.9
0.6
0.3
0
0.72
0.84
0.96
1.08
1.2
54
56
58
60

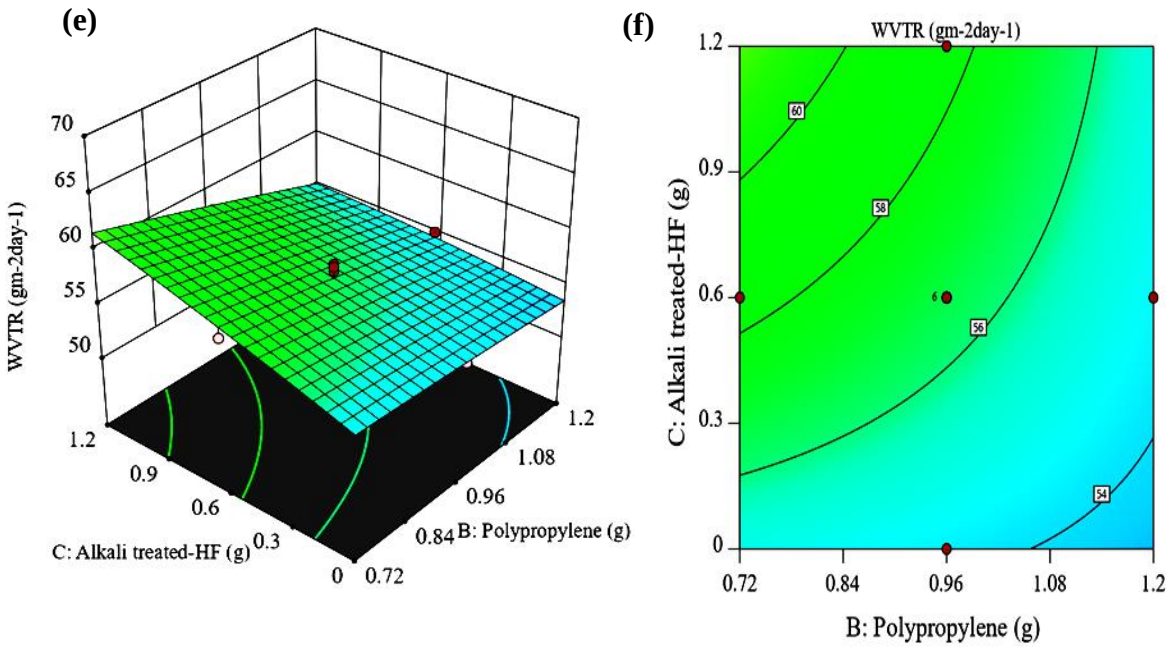

Figure 4.7 Three-dimensional response surface and contour plots of water vapor transmission rate showing the effect of (a) and (b) polypropylene and polyethylene; (c) and (d) alkali treated-HF and polyethylene; (e) and (f) alkali treated-HF and polypropylene.

4.3.3 Optimization of the CCD-RSM model

In order to check the accuracy of the predicted responses provided by RSM, the optimized experiments were carried out with 1.8 g (43.77 wt.%) of PE, 1.112 g (27.04 wt.%) of PP and 1.2 g (29.18 wt.%) of alkali treated-HF. The Predicted output responses are 50 MPa for TS, 119.930 % for EAB and 51.10 g m^{-2} $day^{-1}$for WVTR. The experimental results with output response yield 49.70 for TS, 119.210 % for EAB and 51 $g.m^{-2}.day^{-1}$ for WVTR. Only small percentage errors are found in all output responses, thus, demonstrating reliability of CCD statistical method.

4.3.4 Characterization of the optimized polyethylene/polypropylene/alkali treated-wheat straw bio-composite film

The synthesized PE/PP, PE/PP/NHF and PE/PP/Alkali treated- HF composite films were characterized using SEM, FTIR, XRD, mechanical testing, contact angle, WVTR, WVP and Optical characteristics test.

4.3.4.1 SEM analysis

In order to elucidate the influence of alkali treated- HF on a polymer matrix, scanning electron microscopy for all prepared composite films were performed. The SEM images are depicted in Figure 4.8 with a magnification of 500X in order to visualize the effect of alkali treated-HF on a polymer matrix. The roughness of PE/PP film has been represented in Figure 4.8(a). Figure 4.8(b) depicts the poor dispersion of HF in a film causing some agglomeration of biomass at the surface. Similar observation enlightened by Sánchez-Safont et al., 2018 in their literature. SEM images confirmed the change in surface morphology after blending the polymers with alkali treated-HF (Figure 4.8(c)). SEM images also revealed the increase in roughness after pre-treatment as compared to PE/PP/NHF film. This probably signifies the even distribution of modified-HF in the

polymeric film which is also explained by authors in their published article (Sabetzadeh et al., 2016). This is correlated with a high surface shear force provided by PE/PP/alkali treated-HF film which confirms in the tensile testing.

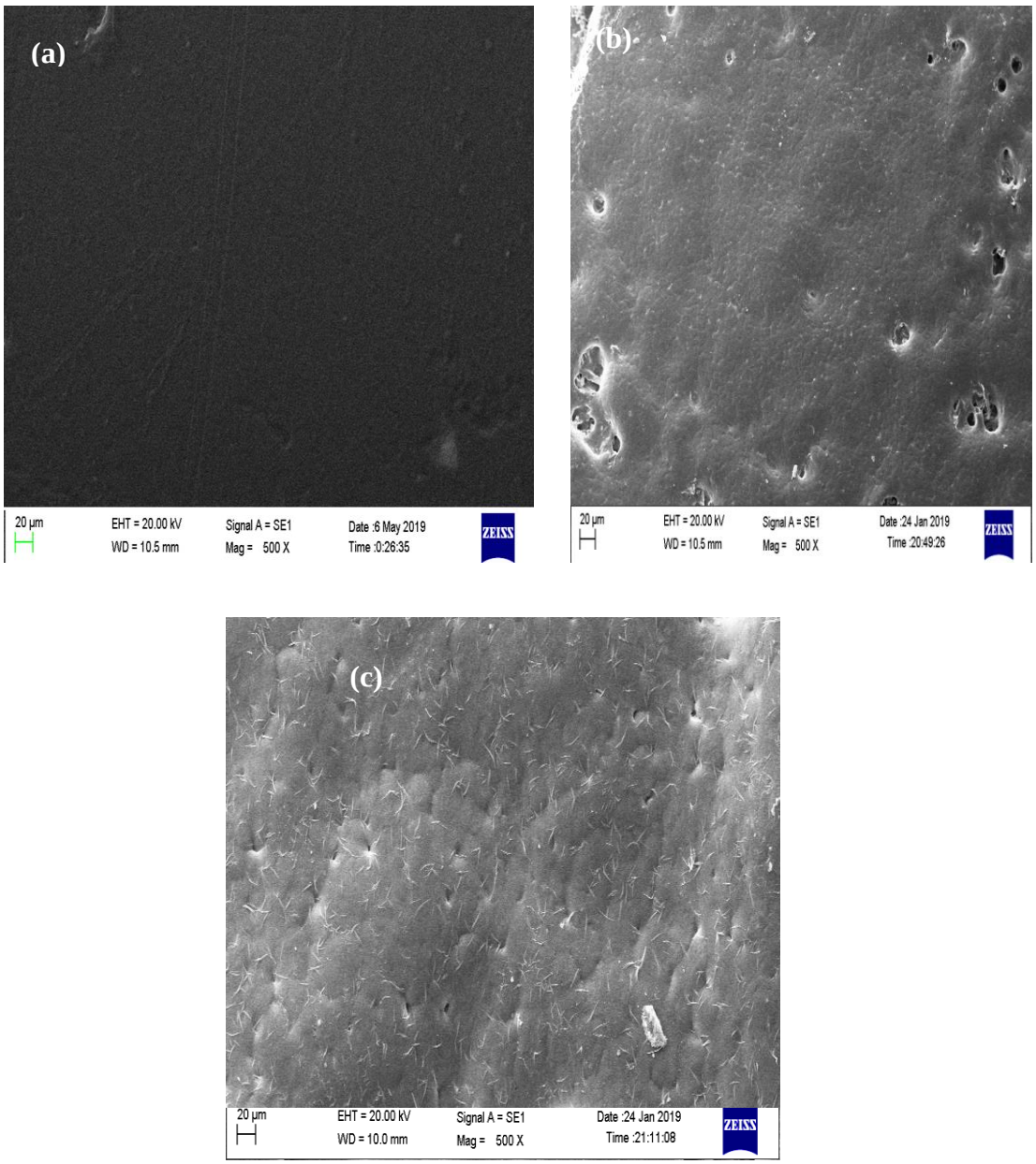

Figure 4.8. SEM analyses for all polymeric composite films (a) PE/PP film (b) PE/PP/native-HF (c) PE/PP/ alkali treated-HF composite films.

4.3.4.2 FTIR analysis

FTIR with ATR mode test was executed to examine the functional groups present in the composite films. Generally, in the FTIR spectroscopy, the absorbance of a specified range of infrared region is measured by the testing films and this absorbance determine the sample's composition by identifying the functional groups present in the film. In this analysis, polymeric films are scanned over the wavelength region at 3500-600 cm^{-1}. FTIR spectra for PE/PP, PE/PP/NHF and PE/PP/alkali treated-HF are shown in Figure 4.9. Peak at 3000-2850 cm^{-1} represents C-H stretching present in the polymeric film. The wavelength range 1470-1450 cm^{-1} exhibits C-H stretching, 1380-1370 cm^{-1} corresponds to CH_2 stretching, and the peak at 1320-1000 cm^{-1} represents C-O stretching present in the film. Peak at 725-675 cm^{-1} represents a =CH out of plane representing the presence of phenyl ring as substitution bands in composite films. The summarized statistics confirm that the testing film is made up of polyethylene and polypropylene. (Gulmine et al., 2002). Peaks at 1300-1375 cm^{-1} assigned to C-H wagging, 3000-2850 cm^{-1} corresponds to CH_2 stretching and 1765-1715 cm-1 assigned to C=O stretching exhibit the existence of agro-waste in the film (Yang et al., 2007).

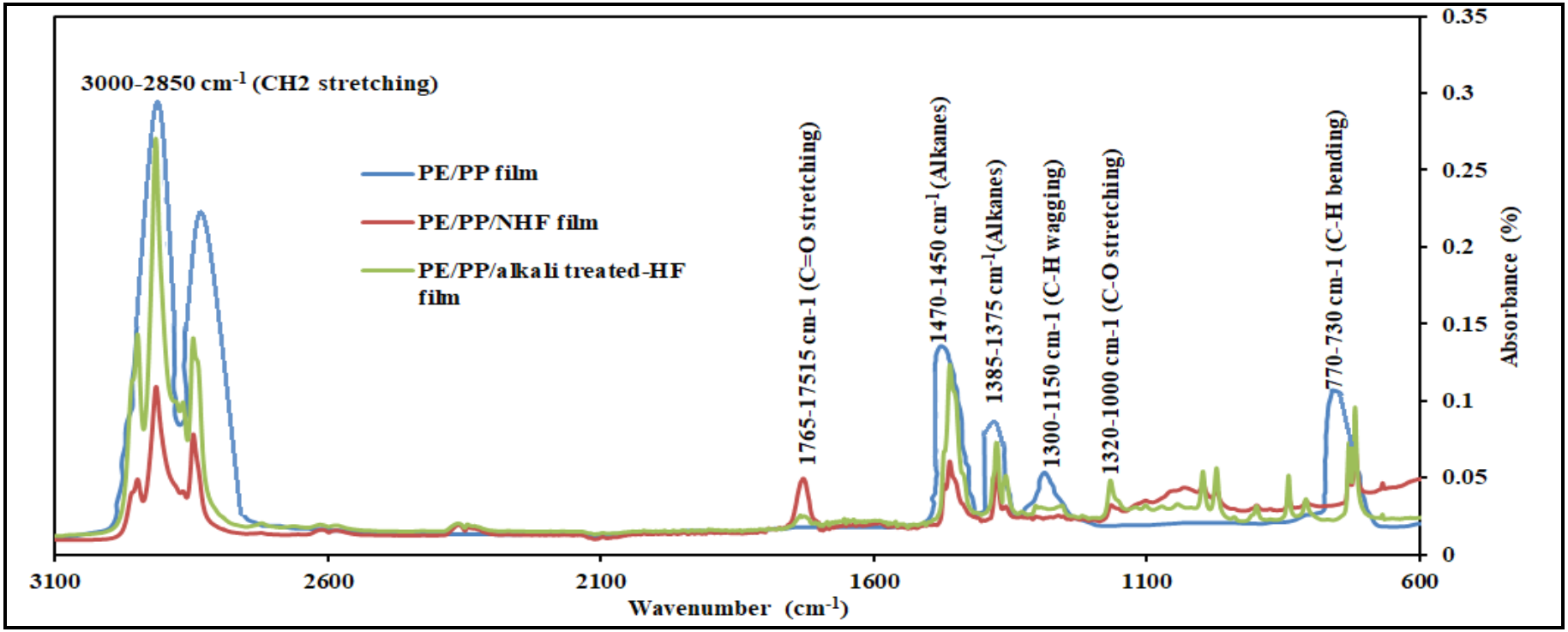

Figure 4.9 FTIR analyses for all polymeric composite films (a) PE/PP film (b) PE/PP/NHF (c) PE/PP/ alkali treated-HF composite films.

4.3.4.3 XRD analysis

XRD analytical technique was used to elucidate the crystalline changes in the polymeric film. XRD analysis is based on the constructive interference of monochromatic X-rays which is originated from the testing samples. Further, this constructive interference provides the information about the crystalline structure or specific arrangement of the atoms in the testing films. XRD spectrums for all prepared composite films are shown in Figure 4.10. Five significant peaks are observed in the XRD spectrum of all films which are nearby 13˚, 16˚, 18˚, 21˚ and 23˚, respectively. XRD patterns showed higher intensity peak at 21.5˚ in PE/PP, 21.48˚ in PE/PP/NHF and 21.38˚ in PE/PP/alkali treated-HF, respectively.

Some shifting of peaks also occurred after biomass addition in the polymer composites. Some decrement is observed in the height of peaks of PE/PP/NHF due to the disturbance in the crystallographic region of a polymer matrix. These results are indicating a poor adhesion found between hemp fiber and the polymer matrix. No prominent variations are visulized in the XRD pattern of PE/PP/alkali treated-HF, exploring the same crystalline pattern as compared with PE/PP. According to Kalia et al., these results are explaining the uniform distribution of treated-HF reinforced polymeric film (Kalia and Vashistha, 2012). Moreover, this may be due to the successful elimination of hemicellulose and lignin from HF. As an outcome, this was showing better compatibility of HF with a polymer matrix assuring a better mechanical strength and higher thermal stability which is also proved in mechanical testing and TGA analysis (Laadila et al., 2017).

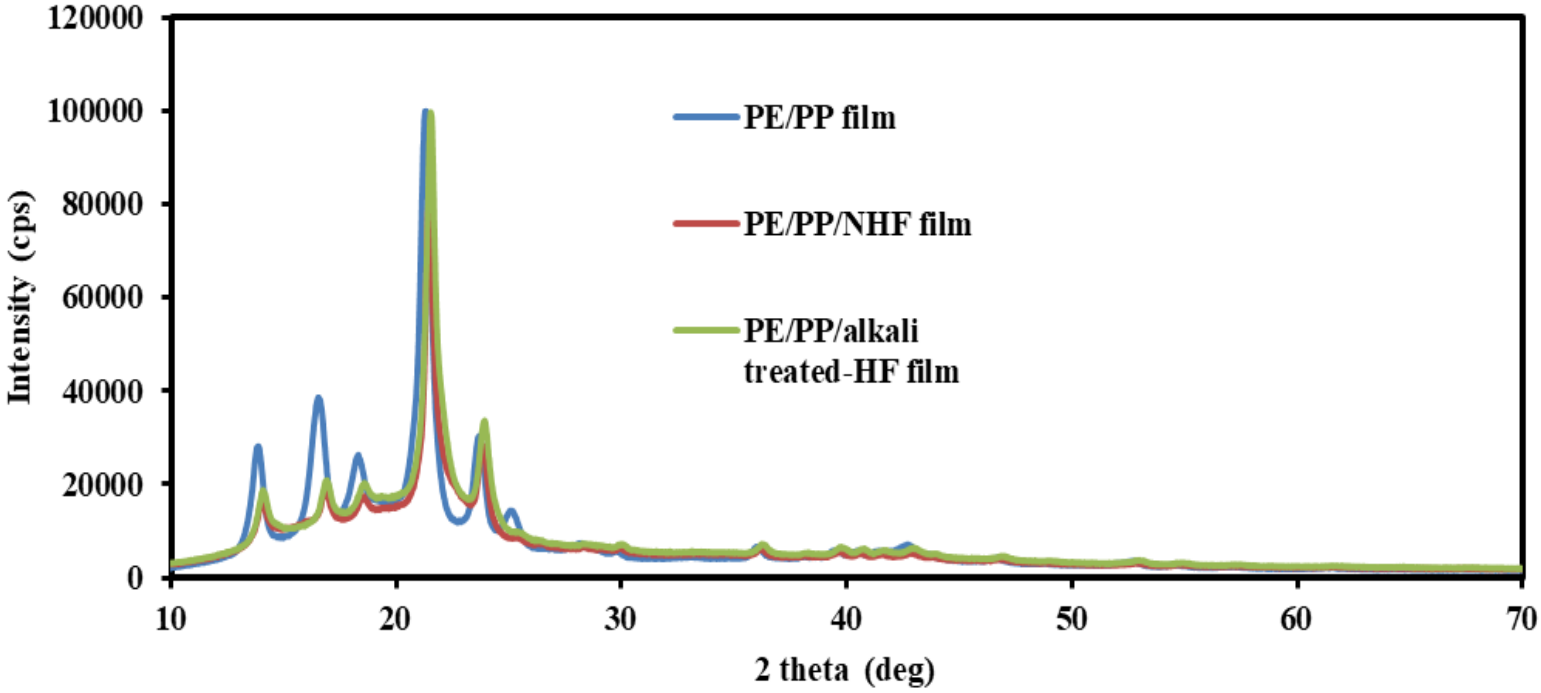

Figure 4.10 XRD analyses for all polymeric composite films (a) PE/PP film (b) PE/PP/NHF (c) PE/PP/ alkali treated-HF composite films.

4.3.4.4 TGA analysis

The TGA curves for all prepared films have been presented in Figure 4.11. The thermal decompositions for the three films show many steps in the curve revealing the existence of different kind of materials decomposed at different temperatures. Initial degradation starts at around 150°C and ends at 234°C with 2% weight loss. Major degradation starts at around 342 °C for PE/PP with 2% weight loss, 332 ^{O}C for real packaging film with 3% weight loss, 237 °C for PE/PP/NHF with 2% weight loss and 288 °C for PE/PP/alkali treated-HF with 2% weight loss. Moreover, thermal degradation ends at around 490 °C for PE/PP with 19% weight loss, 425 ^{O}C for real packaging film with 20% weight loss, 426 °C for PE/PP/NHF with 35% weight loss and 428 °C for PE/PP/alkali treated-HF with 24 % weight loss. Another degradation ends at 490 °C for PE/PP with 88% weight loss, 509 ^{O}C for real packaging film with 89 % weight loss, 474 °C for PE/PP/NHF with 77% weight loss and 488 °C for PE/PP/alkali treated-HF with 85 % weight loss in thermal degradation graph.

Initial degradation of PE/PP/NHF exhibits a de-bonding present between the PP/PE and NHF. Seggiani et al., 2017 stated similar results in their published article. The main degradation for films signifies the degradation of biomass, polyethylene and polypropylene in a composite film. There is some enhancement in the thermal stability of treated fiber based composite film as compared to native fiber based composite film due to the even distribution of treated biomass in polymeric matrix. The authors explained equivalent outcomes in their published literature (Perumal et al., 2018).

Thus, it can be concluded that the addition of NaOH treated-HF in a polymer matrix shifts the thermal degradation towards the higher temperature. There are some inert chemical materials also found in a TGA thermo-gram in biomass-based composite film

after a temperature of 475 °C. As is evident from the results, there is an improvement in the thermal stability of PE/PP/alkali treated-HF film which is comparable with the PE/PP film and real packaging film. This signifies the successful enhancement of cellulose percentage in hemp fiber after alkali treatment and its outcome in better adhesion between the alkali treated-HF and polymer matrix (Dixit and Yadav, 2019b).

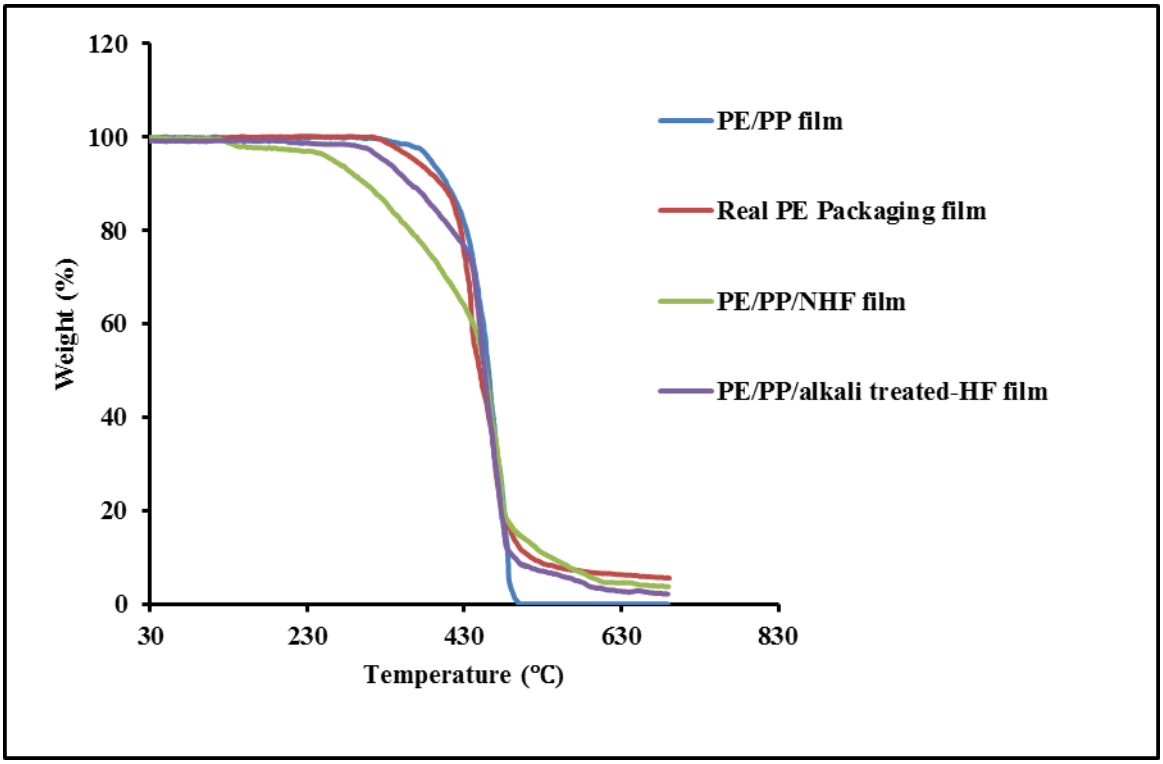

Figure 4.11 TGA analyses for all polymeric composite films (a) PE/PP film (b) Real packaging (c) PE/PP/NHF (d) PE/PP/ alkali treated-HF composite films.

4.3.4.5 Mechanical test

Mechanical stability plays an important role in order to synthesize the high-quality packaging film. Tensile strength expresses the maximum force that the packaging film can withstand before failure. Elongation limit reveals the flexibility of the film before failure in tensile test. In order to examine the mechanical strength of the composites, tensile and elongation at break (%) tests for films were conducted. The TS of PE/PP, real PE packaging, real polyester packaging, PE/PP/NHF and PE/PP/alkali treated-HF films are 46.5 MPa, 29.07 MPa, 25.50 MPa, 37 MPa, and 49.70 MPa, respectively (Table 4.7). Moreover, the flexibility of the prepared films is 122.05%, 124.92%, 117.37%, 116.90% and 119.210 %, respectively.

The film, as synthesized from HF, shows an absence of strong adhesion between polymer and fiber resulting in poor mechanical stability. The tensile strength of alkali treated-HF reinforced polymer composite is increased from 37 to 49.70 MPa as compared to native fiber based polymeric film. This result is associated with the suitability of treated fiber in the polymer matrix. Moreover, tensile strength of treated fiber based film is much higher as compared to real PE or polyester packaging films. Nyambo et al., 2011 has also stated the same outcomes in their research article.

The percentage of elongation is also decreased after biomass addition in a polymer matrix. A notable increment in flexibility is also observed after treated-HF blended in the film. The flexibility of treated-HF based film is increased from 116.90% to 119.210%. It is clear that there is benchmark improvement in tensile strength with moderate flexibility after blending of alkali treated-HF in composites showing reduction in recalcitrance nature of biomass (Sánchez-Safont et al., 2018).

These outcomes show the strong interfacial interaction between the alkali treated-HF and polymers. Therefore, it can be assured that alkali treated-HF reinforced film is the promising replacement of synthetic films in packaging applications (Perumal et al., 2018).

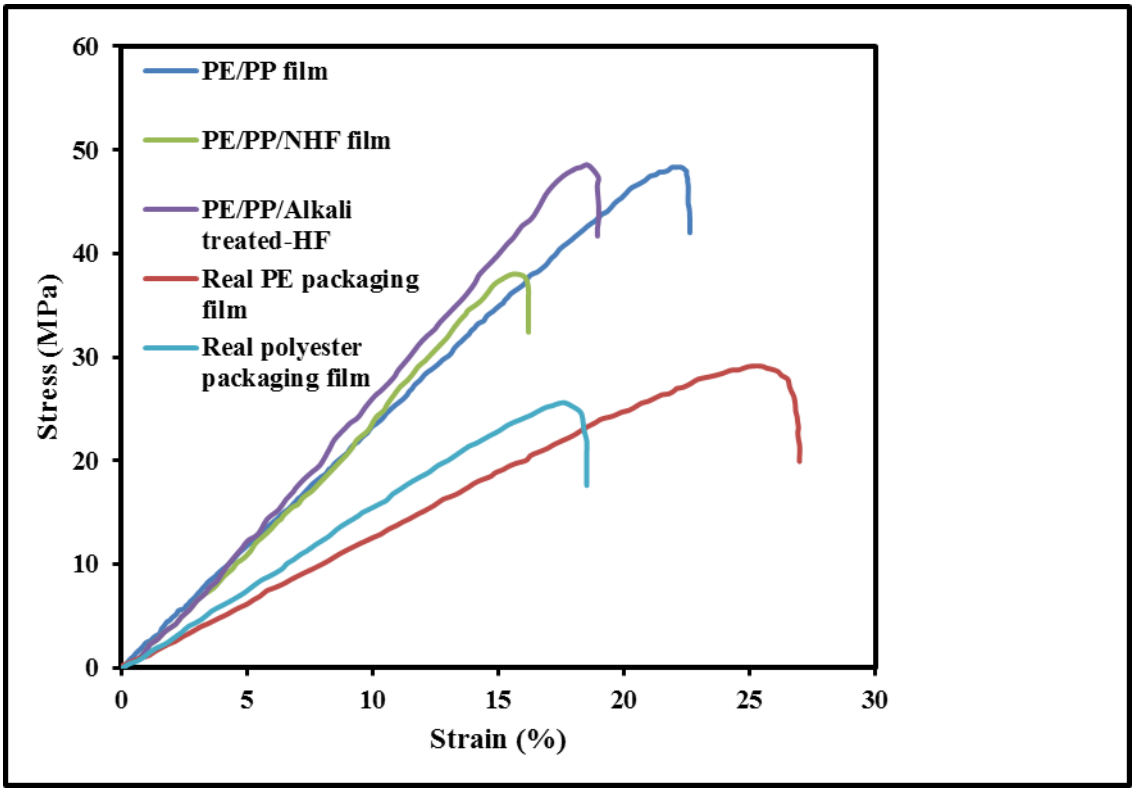

Figure 4.12 Stress vs. strain curve for polymeric composite films (a) PE/PP film (b) Real PE packaging (c) real polyester packaging (d) PE/PP/NHF (e) PE/PP/ alkali treated-HF composite films.

Table 4.7 Tensile stress, Yield strength, Elongation at break and Young modulus for all polymeric composite films.

Film	Tensile stress at break (MPa)	Yield strength (MPa)	Elongation at break (%)	Young Modulus (MPa)
PE(60 wt.%)/ PP (40 wt.%)	46.5	45.34	122.05	210.88
Real PE packaging	29.07	28.45	124.92	116.65
Real polyester packaging	25.50	25.14	117.37	146.80
PE (43.77 wt.%)/ PP (27.04 wt.%)/ native-HF (29.18 wt.%)	37	35.78	116.90	218.93
PE (43.77 wt.%)/ PP (27.04 wt.%)/Alkali treated-HF(29.18wt.%)	49.70	42.62	119.210	258.71

4.3.3.6 Contact angle

Contact angle measurement principal is based on the surface tension between the liquid-solid interfaces. Contact angle test explores wettability of the surface of the film. In this test, small droplet is allowed to fall on the testing surface and the shape of the droplet of distilled water is observed on the surface with time. In addition, the shape of the droplet does not change with time showing hydrophobic characteristics of the film. Contact angles for all synthesized and real packaging films are shown in Table 4.8. The water contact angle values of polymeric film, real packaging, real polyester packaging, native-fiber based polymeric film and modified-fiber based polymeric film are 121°, 120°, 60 ^{o}, 91° and 119 ^{o}, respectively.

Based on the results, all synthesized polymeric composite films are higher contact angle as compared to real polyester packaging film. The contact angle value increases by 18° in alkali treated-HF based polymer matrix assuring its water proofing quality.

Generally, a higher contact angle ≥ 90° signifies that the tension force between film and water is very less. This reveals the hydrophobic nature of the film. So probably, alkali treated-HF reinforced PE/PP matrix depicts appropriateness for green applications (Tang et al., 2009).

4.3.3.7 WVP test

WVP and WVTR are one of the important parameters for checking the barrier property of the packaging film. WVP generally expresses the water vapor migration through the film using wet cup method. The commonly used distilled water to maintain 100% relative humidity inside the wet cup chamber. The mass loss of water from a wet cup chamber over the period of time is recorded and WVP and WVTR at the steady-state region at a certain temperature with fixed relative humidity are determined. WVP experiments were carried out for all prepared films and the results are represented in Table 4.8. WVTR and WVP for real polyethylene packaging films are 45.1 $g.m^{-2}.day^{-1}$ and 2.37E-11 $g.m^{-1}.Pa^{-1}.s^{-1}$, respectively which is showing a moisture-resistant nature of the film. On the other hand, WVP for PE/PP, real polyester packaging, native- hemp fiber reinforced polymeric film and treated- hemp fiber reinforced polymeric film are 2.50E-11, 3.13E-10, 6.34E-11 and 2.69 E-11 $g.m^{-1}.Pa^{-1}.s^{-1}$, respectively.

Due to the hydrophilicity of PE/PP/NHF and real polyester packaging films, WVTR and WVP are very high as compared to real polyethylene packaging and PE/PP film. It can be the better water affinity of CH group which allowed water molecules transport through the film. The authors explained equivalent outcomes in their published articles (Sánchez-Safont et al., 2018). But there are decrement in the value of WVTR and WVPR after alkali treatment because of the possibility of the better dispersion of treated-HF in the polymer matrix (Tănase et al., 2015). Low WVP makes the alkali

treated-HF based polymeric film more suitable for water resistant packaging applications.

4.3.3.8 Dart Impact test

Impact strength is an important property in terms of packaging film characteristics. Impact strength generally exhibits the ability of a film to withstand a sudden load applied to the film and observes the accessibility of the film for packaging industries. To evaluate the impact strength of all synthesized and real packaging film, a free-falling dart impact method is used. Dart impact test is helpful to understand the film's impact resistance according to ASTMD1709. The thickness of the film is 0.25±0.03 mm. In this test, a dart of different weights is dropped perpendicular from a height of 43 cm to the surface of the polymeric film in order to calculate the impact strength of the material until it partially or completely breaks the film. Dart impact energy, dart impact strength, striking velocity before impact and dart failure weight for PE/PP, real PE packaging, real polyester packaging, PE/PP/NHF and PE/PP/alkali treated-HF film is shown in Table 4.8. The dart impact strength for PE/PP, real polyethylene packaging, real polyester packaging, PE/PP/NHF and PE/PP/alkali treated-HF films is 2069 J/m, 2052 J/m, 1453 J/m, 1624 J/m and 2034 J/m, respectively. There is a decrease in impact strength after incorporation of NHF in PE/PP matrix. This shows a poor interfacial interaction between the biomass and polymer which is confirmed in tensile test. Alkali treatment enhances the impact strength by 25% which is comparable with real polyethylene packaging film for green packaging applications.

4.3.3.9 Optical characteristics test

Transparency is an important characteristic of the film for packaging applications. Optical characteristics test is a prominent method to measure the transparency of the film. In this optical test, the visible light transmission rate through all synthesized and real packaging films was investigated. Table 4.8 depicts a light transmission rate through polymeric composite films over the wavelength range of 400-800 nm. The light transmission rate of PE/PP/NHF film is 12% at 800 nm that is higher as compared to real polyester packaging film. So probably, it can be said that the light transmission rate of PE/PP/NHF film is less as compared to PE/PP over a visible wavelength range. The transparency of PE/PP/alkali treated-HF is 20% at 800 nm revealing even distribution of alkali treated-HF in the film. Uniform distribution of biomass signified the existence of strong adhesion between the NaOH treated-HF and the polymer matrix (El Achaby et al., 2017). Zeng et al., 2005 stated that the uniform distribution of filler in the matrix was correlated with the improvement in transparency. So, it can be concluded from optical test results that NaOH treated-HF based composite film has hazing transparency.

Table 4.8 Contact angle, Dart impact velocity, Dart impact failure weight, WVTR, WVP and light transmission rate for all polymeric composite films.

Film	**Contact angle (deg)**	**Dart Impact velocity before strike (m/s)**	**Dart Impact Failure weight (g)**	**Dart Impact strength (J/m)**	**WVTR ($g.m^{-2}$ day^{-1})**	**WVP ($g.m^{-1}.Pa^{-1}.s^{-1}$)**	**Light transmission rate through a different visible wavelength range (nm)**		
							400	**600**	**800**
PE/PP	121°±4	2.93	121	2069	47.50	2.50E-11	30.5±0.02	34.30±0.01	41.20±0.02
Real packaging	120°±1	2.93	120	2052	45.1	2.37E-11	90±0.015	92±0.02	95±0.01
Real polyester packaging	60±4	2.93	85	1453	268.86	3.13E-10	1.76±0.08	1.90±0.06	1.96±0.05
PE/PP/NHF	91°±4	2.93	95	1624	120.2	6.34E-11	9± 0.02	11± 0.04	12±0.03
PE/PP/ Alkali treated-HF	119°±2	2.93	119	2034	51	2.69E-11	15±0.05	18±0.04	20±0.07

4.4 Conclusions

In summary, polyethylene, polypropylene and alkali treated-hemp fiber independent variables were used for fabricating an optimized biocomposite film carried out by CCD-RSM. The optimized responses such as mechanical strength, flexibility and WVTR provided by model were 47.20 MPa, 119.930 % and 51 $g.m^{-}2.day^{-1}$, respectively. Moreover, these results are similar with experimental result presenting the correctness of CCD-RSM model. Further, the film synthesized from optimized independent factors was characterized using tensile test, TGA, contact angle, impact test, water vapor permeability, and transparency test. TGA analysis signified that there was an improvement in the thermal stability of alkali treated-HF based polymer composite. Benchmark decrement in WVP and WVTR revealed that the composite made by alkali treated-HF was showing suitability for water-resistant packaging applications. Higher contact angle of PE/PP/alkali treated-HF exhibited a water-resistant quality of the film. Comparable mechanical strength with a PE/PP composite film, moderate impact strength and hazing transparency assured an excellent adhesion between treated-HF and the polymer matrix. The observed improvement in thermal stability, better mechanical strength, hydrophobicity, and low WVPR encourage the researchers to synthesize biocomposites for sustainable packaging applications.